Symmetry Chirp Spread Spectrum Modulation Used in LEO Satellite Internet of Things

Yubi Qian, Lu Ma, and Xuwen Liang

***Abstract*— With the development of Internet of Things (IoT), the world gradually moves toward the interconnection of all things. In terrestrial networks, narrowband-IoT and Long Rage (LoRa) are used widely in the IoT industry. For low-earth-orbit (LEO) satellites, they have a lot of conspicuous advantages, such as broader coverage and lower construction cost. In this letter, we place emphasis on the application of LoRa-related technologies to LEO satellite communication systems, and the modulation is the prior research. Chirp spread spectrum (CSS) modulation is the most important technology in LoRa. Therefore, the research of CSS modulation used in the satellite IoT is imperative.**

***Index Terms*— IoT, LEO Satellite, NB-IoT, LoRa, CSS, SCSS.**

I. Introduction

INTERNET of Things(IoT) [1] is the timely topic in the field of current communication and characterized by massive terminals, low power consumption, low data rate and low duty cycle. In low-earth-orbit(LEO) Satellite communications, Time Delay(TD) and Doppler Frequency Shift(DFS) are much bigger than those in the ground communications. Spread spectrum communication has anti-interference and anti-multipath characteristics and Direct Sequence Spread Spectrum(DSSS) [2] has been widely used in the satellite communication. However, Chirp Spread Spectrum(CSS) has never been used in the satellite communication for low-data-rate transmission, but LoRa(Long Range) [3], [4] has successfully applied it to Low-Power Wide-Area Network (LPWAN) in the ground communication systems. This letter is about the research on the application of CSS to the LEO satellite communication. First and foremost, we need to find the correlation between chirp signals, because the correlation plays a directive role in the coherent demodulation, through understanding code and DFS acquisition in DSSS [5].

In order to simplify the analyses in Section III and IV, two kinds of integrals [8] are introduced in the Section II. In Section III, We give the description of CSS(LoRa modulation) and we find that this kind of CSS cannot be used in satellite communication. Therefore, Symmetry Chirp Spread Spectrum(SCSS) is put forward in Section IV. According to the characteristics of SCSS, there are two kinds of modulation, Frequency and Phase Symmetry Chirp Spread Spectrum(FSCSS and PSCSS) specified in Section V. Finally, the conclusion of all the letter is in Section VI.

Manuscript received July 23, 2018; accepted August 18, 2018. Date of publication August 23, 2018; date of current version November 12, 2018. The associate editor coordinating the review of this paper and approving it for publication was L. Mucchi. *(Corresponding author: Yubi Qian.)*

Y. Qian is with the Shanghai Institute of Microsystem and Information Technology, Chinese Academy of Sciences, Shanghai 100049, China, also with the Shanghai Engineering Center for Microsatellites, Chinese Academy of Sciences, Shanghai 100049, China, and also with the University of Chinese Academy of Sciences, Beijing 100049, China (e-mail: yubiqian@foxmail.com).

L. Ma is with Shanghai SpaceOK Aerospace Technology Co., Ltd., Shanghai 201802, China (e-mail: e_wqs@hotmail.com).

X. Liang is with the Shanghai Engineering Center for Microsatellites, Chinese Academy of Sciences, Shanghai 100049, China (e-mail: 18217631362@163.com).

Digital Object Identifier 10.1109/LCOMM.2018.2866820

II. Symbol Description and Related Integrals

A. Symbol Description

We define some symbols in this letter. R_s denotes the symbol rate(corresponding symbol period is T_s, and symbol rate is equal to bit rate in this letter). Transmission bandwidth of one channel is $B(T = \frac{1}{B})$ and spread factor is $SF(SF = 6, 7, 8 \ldots 12$ in LoRa, spreading gain $G = 2^{SF})$. The relation between transmission bandwidth and symbol rate is $BT_s = 2^{SF}$. As for integral range, $T_a, T_b \in [0, T_s]$ and $T_b > T_a$. E_s represents the energy of one symbol, and its power is $p = \frac{E_s}{T_s}$. Start frequency of chirp signals $b_k = \frac{B_k B}{2^{SF}}, B_k \in \{0, 1, 2, \ldots 2^{SF} - 1\}, A_k = 2^{SF} - B_k$.

B. Chirp Signals for the Same Chirp Rate

$$\begin{aligned} I_{CSSCR} &= p\int_{T_a}^{T_b} e^{j\pi\mu t^2 + j2\pi f_1 t}(e^{j\pi\mu(t-\tau)^2 + j2\pi f_2(t-\tau)})^* dt \\ &= pe^{-j\varphi} sinc[(\mu\tau + (f_1 - f_2))(T_b - T_a)](T_b - T_a) \end{aligned} \tag{1}$$

where

$$\varphi = \pi\mu\tau(\tau - (T_a + T_b)) + 2\pi f_2\tau - \pi(f_1 - f_2)(T_a + T_b)$$

$$sinc(x) = \frac{sin(\pi x)}{\pi x}$$

τ is time delay, and μ is the chirp rate. We get a result: when $(\mu\tau + (f_1 - f_2))(T_b - T_a) = 0 \Rightarrow \hat{\tau} = \frac{(f_2 - f_1)}{\mu}$, then $max(|I_{CSSCR}|) = p(T_b - T_a)$. When we bring $\hat{\tau}$ back to (1),

$$I_{CSSCR} = p(T_b - T_a)e^{\frac{-j\pi(f_1^2 - f_2^2)}{\mu}} \tag{2}$$

From the result of Equation(1), cross-correlation of two chirp signals with the same chirp rate can get the maximum value only when their time-frequency curves overlap by changing τ.

C. Chirp Signals for the Inverse Chirp Rate

$$\begin{aligned} I_{CSICR} &= p\int_{T_a}^{T_b} e^{j\pi\mu t^2 + j2\pi f_1 t}(e^{-j\pi\mu(t-\tau)^2 + j2\pi f_2(t-\tau)})^* dt \\ &= pe^{j(\pi\mu\tau^2 + 2\pi f_2\tau)} \int_{T_a}^{T_b} e^{j2\pi\mu t^2} e^{-j2\pi(\mu\tau - (f_1 - f_2))t} dt \end{aligned} \tag{3}$$

As shown in (3), it is difficult to find this integral result for no elementary primitive function of $e^{j2\pi\mu t^2}$. Equation(3) can be considered as the amplitude value at $f = \mu\tau - (f_1 - f_2)$ after its Fourier Transform according to Fourier Transform Formula. let $\mu = \frac{B}{T_s}$. When we calculate Fast Fourier Transform(FFT) of its discrete series with MATLAB, the amplitude value is very small and becomes smaller as SF increases when keeping transmission bandwidth B invariable. Hence, the value of integral can be very small, $|I_{CSICR}| \ll p(T_b - T_a)$.

III. Chirp Spread Spectrum

LoRa modulation [6] is a kind of frequency shift chirp modulation [7]. When we take the LoRa into account, we find that LoRa can distinguish the information by different values of start frequency of chirp signals. There are two important equations in [6].

$$s(nT_s) = \sum_{h=0}^{SF-1} w(nT_s)_h \cdot 2^h \tag{4}$$

$$c(nT_s + kT) = \frac{1}{\sqrt{2^{SF}}} e^{j\frac{2\pi}{2^{SF}}[(s(nT_s)+k) \bmod 2^{SF}]k} \tag{5}$$

Where $n \in \{0, 1, 2 \ldots 2^{SF} - 1\}$, $k \in \{0, 1, 2 \ldots 2^{SF} - 1\}$

As shown in (4), it can be explained that it transfers the 2^{SF} binary bits into a decimal number in a period T_s, and $s(nT_s)$ determines the start frequency of chirp signals. But in LEO satellite IoT, we cannot use this kind of CSS to achieve multiple access communication. In this letter, we use different values of start frequency to represent respective signals transmitted by different terminals. Then we give the analyses of CSS under the situation of multiple terminals.

A. Frequency

Because the frequency of CSS signal is linear with the time, for terminal k, it can be denoted as,

$$f_k(t) = (b_k + \frac{B}{T_s}t) \bmod B \tag{6}$$

B. Time-Domain Continual Signal

According to the relation between frequency and phase, we get time-domain continual signal,

$$s_k(t) = \sqrt{\frac{E_s}{T_s}} e^{j2\pi \cdot \int_o^t f_k(t)dt} \tag{7}$$

Bring (6) into (7) and get the following results,

$$s_k(t) = \begin{cases} s1_k(t) = \sqrt{\frac{E_s}{T_s}} e^{j2\pi(\frac{B}{2T_s}t^2 + b_k t)}, & 0 \le t < T_k \\ s2_k(t) = \sqrt{\frac{E_s}{T_s}} e^{j2\pi(\frac{B}{2T_s}t^2 + b_k t - Bt)}, & T_k \le t < T_s \end{cases} \tag{8}$$

Where $T_k = (1 - \frac{b_k}{B})T_s = A_k T$.

C. Cross-Correlation

$$R(\tau, k_1, k_2) = \int_0^{T_s} s_{k_2}(t) s^*_{k_1}(t - \tau)dt \tag{9}$$

In this, $\mu = \frac{B}{T_s}$. As shown in Fig.1, suppose that $b_{k_1} \ge b_{k_2}, B_{k_1} \ge B_{k_2}, A_{k_1} \le A_{k_2}$ and vice versa according to $R(\tau, k_1, k_2) = R^*(-\tau, k_2, k_1)$. In our study, we want to find the maximum $R(\hat{\tau}, k_1, k_2)$. According to (1), (9) and Fig.1, there are two special values of $\hat{\tau}$. When

$$\hat{\tau}_1 = \frac{(b_{k_1} - b_{k_2})T_s}{B}$$

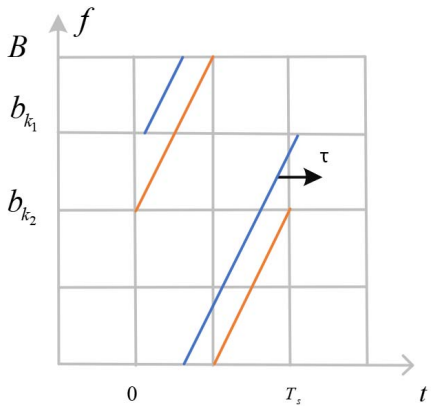

Fig. 1. Time-Frequency of CSS for terminal k_1 and terminal k_2.

the cross-correlation is calculated in (10).

$$\begin{aligned} R_{CSS}(\hat{\tau}_1, k_1, k_2) &= \int_{\hat{\tau}_1}^{A_{k_2}T} s1_{k_2}(t) s1^*_{k_1}(t - \hat{\tau}_1)dt \\ &\quad + \int_{A_{k_2}T}^{T_s} s2_{k_2}(t) s2^*_{k_1}(t - \hat{\tau}_1)dt \\ &= E_s \frac{T_s - \hat{\tau}_1}{T_s} e^{-\frac{j\pi T_s}{B}(b^2_{k_2} - b^2_{k_1})} \end{aligned} \tag{10}$$

Similarly, according to Fig.1, When

$$\hat{\tau}_2 = \hat{\tau}_1 - T_s = \frac{(b_{k_1} - b_{k_2} - B)T_s}{B}$$

recalculate the cross-correlation,

$$R_{CSS}(\hat{\tau}_2, k_1, k_2) = E_s \frac{T_s + \hat{\tau}_2}{T_s} e^{-\frac{j\pi T_s}{B}(b^2_{k_2} - b^2_{k_1})} \tag{11}$$

$$|R_{CSS}(\hat{\tau}_1, k_1, k_2)| + |R_{CSS}(\hat{\tau}_2, k_1, k_2)| = E_s \tag{12}$$

Especially, when $b_{k_1} = b_{k_2}$, $\hat{\tau}_1 = 0$, thus we can get the auto-correlation,

$$|R_{CSS}(\hat{\tau}_1, k_1, k_2)| = E_s \tag{13}$$

D. Results of Chirp Spread Spectrum

According to (10), (11), and (12), we get two results:

1) When $|b_{k_1} - b_{k_2}|$ is close to 0 or B, the maximum cross-correlation between two signals is big and its value is close to E_s.
2) $max(|R_{CSS}(\hat{\tau}, , k_1, k_2)|) \ge 0.5E_s, \forall b_{k_1}, b_{k_2}$.

Due to 1), 2), it is difficult to demodulate the signals from multiple terminals in one T_s for big cross-correlation, when $|b_{k_1} - b_{k_2}|$ is close to 0 or B.

IV. Symmetry Chirp Spread Spectrum

In order to solve the problem of big cross-correlation, we introduce SCSS in this section. From the inspiration of primary chirp signals [9], positive chirp rate signal represents binary '1', while negative chirp rate signal represents binary '0'. Because the cross-correlation between these two kinds of signals is small(they are approximately orthogonal), which can be deduced by (3). Based on these, SCSS is introduced in next subsections.

A. Frequency

There are two kinds of symmetry chirp signals and their each symbol period T_s is divided in half. Negative and positive chirp rate signal alternate at each half period.

$$f_k(t) = \begin{cases} (\frac{2B}{T_s}t + b_k) \bmod B, & t < \frac{T_s}{2} \\ (-\frac{2B}{T_s}(t - \frac{T_s}{2}) + b_k) \bmod B, & t < T_s \end{cases}$$
$$= \begin{cases} \frac{2B}{T_s}t + b_k, & t < T_k \\ \frac{2B}{T_s}t + b_k - B, & t < \frac{T_s}{2} \\ -\frac{2B}{T_s}t + b_k + B, & t < T_s - T_k \\ -\frac{2B}{T_s}t + b_k + 2B, & t < T_s \end{cases} \quad (14)$$

Or,

$$f_k(t) = \begin{cases} (-\frac{2B}{T_s}t + b_k) \bmod B, & t < \frac{T_s}{2} \\ (\frac{2B}{T_s}(t - \frac{T_s}{2}) + b_k) \bmod B, & t < T_s \end{cases}$$
$$= \begin{cases} -\frac{2B}{T_s}t + b_k, & t < T'_k \\ -\frac{2B}{T_s}t + b_k + B, & t < \frac{T_s}{2} \\ \frac{2B}{T_s}t + b_k - B, & t < T_s - T'_k \\ \frac{2B}{T_s}t + b_k - 2B, & t < T_s \end{cases} \quad (15)$$

Where $T_k = (1 - \frac{b_k}{B})\frac{T_s}{2} = \frac{A_k T}{2}, T'_k = \frac{b_k}{B}\frac{T_s}{2} = \frac{B_k T}{2}$

B. Time-Domain Continual Signal

According to (7), (14), and (15), time-domain continual signals are shown,

$$s_k(t) = \sqrt{\frac{E_s}{T_s}} \begin{cases} s1_k(t) = Se1_{b_k}(t), & t < T_k \\ s2_k(t) = (-1)^{A_k} Se1_{b_k}(t) e^{-j2\pi Bt}, & t < \frac{T_s}{2} \\ s3_k(t) = (-1)^{A_k} Se2_{b_k}(t) e^{j2\pi Bt}, & t < T_s - T_k \\ s4_k(t) = Se2_{b_k}(t) e^{j4\pi Bt}, & \leq t < T_s \end{cases} \quad (16)$$

Or,

$$s'_k(t) = \sqrt{\frac{E_s}{T_s}} \begin{cases} Se2_{b_k}(t), & t < T'_k \\ Se2_{b_k}(t) e^{j2\pi Bt}(-1)^{B_k}, & t < \frac{T_s}{2} \\ Se1_{b_k}(t) e^{-j2\pi Bt}(-1)^{B_k}, & t < T_s - T'_k \\ Se1_{b_k}(t) e^{-j4\pi Bt}, & t < T_s \end{cases} \quad (17)$$

Where

$$Se1_k(t) = e^{j2\pi(\frac{B}{T_s}t^2 + b_k t)}, \quad Se2_k(t) = e^{j2\pi(-\frac{B}{T_s}t^2 + b_k t)}$$

C. Cross-Correlation

In this, $\mu = \frac{2B}{T_s}$. Let $b_{k_1} \geq b_{k_2}$, then $B_{k_1} \geq B_{k_2}, A_{k_1} \leq A_{k_2}$ and we use $s_k(t)$ to analyze cross-correlation. According to (1), (2), (3), (9), (16) and Fig.2, there are two special values

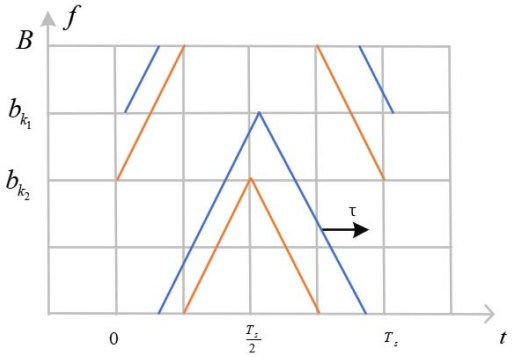

Fig. 2. Time-Frequency of SCSS for terminal k_1 and terminal k_2.

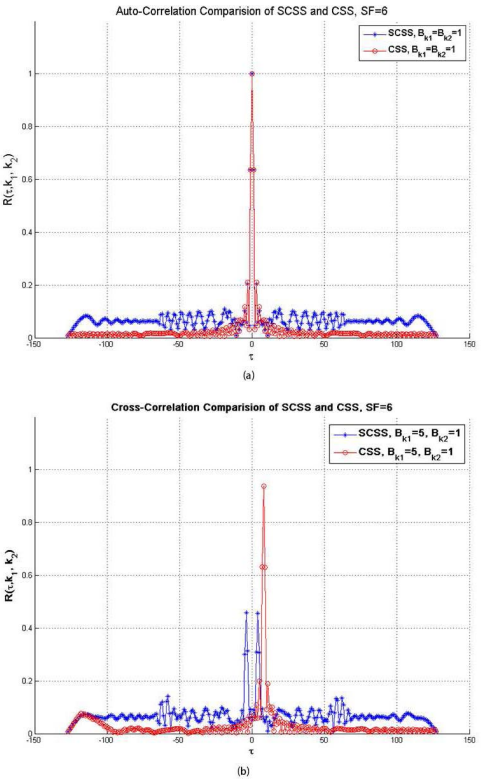

Fig. 3. Auto-correlation and Cross-Correlation Comparison of SCSS and CSS.

of $\hat{\tau}$. When

$$\hat{\tau}_1 = \frac{(b_{k_1} - b_{k_2})T_s}{2B}$$

two time-frequency curves of b_{k_1} and b_{k_2} symmetry chirp signals overlap, so as to get the maximum value. In this study, we do approximate algorithm and ignore non-overlapped integral range,

$$R_{SCSS}(\hat{\tau}_1, k_1, k_2) = \int_0^{T_s} s_{k_2}(t) s^*_{k_1}(t - \hat{\tau}_1) dt$$
$$\approx \int_{\hat{\tau}_1}^{\frac{A_{k_2}T}{2}} s1_{k_2}(t) s1^*_{k_1}(t - \hat{\tau}_1) dt$$
$$+ \int_{\frac{A_{k_2}T}{2}}^{\frac{T_s}{2}} s2_{k_2}(t) s2^*_{k_1}(t - \hat{\tau}_1) dt$$
$$= E_s \frac{(T_s - 2\hat{\tau}_1)}{2T_s} e^{-\frac{j\pi T_s}{2B}(b^2_{k_2} - b^2_{k_1})} \quad (18)$$

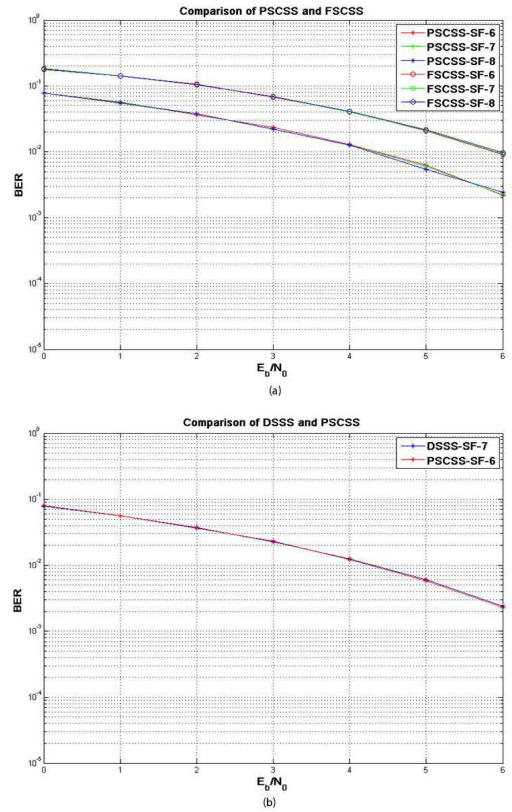

Fig. 4. Uncoded E_b/N_0-BER of Binary FSCSS, Binary PSCSS and DSSS in the AWGN Channels.

Similarly, As shown in Fig.2, When

$$\hat{\tau}_2 = -\hat{\tau}_1 = \frac{(b_{k_2} - b_{k_1})T_s}{2B}$$

recalculate the cross-correlation,

$$R_{SCSS}(\hat{\tau}_2, k_1, k_2) \approx E_s \frac{(T_s + 2\hat{\tau}_2)}{2T_s} e^{-\frac{j\pi T_s}{2B}(b_{k_2}^2 - b_{k_1}^2)} \quad (19)$$

According to (18) and (19), $|R_{SCSS}(\hat{\tau}, k_1, k_2)| < 0.5E_s$ when $b_{k_1} \neq b_{k_2}$. Especially, when $b_{k_1} = b_{k_2} \Rightarrow \hat{\tau}_1 = \hat{\tau}_2 = 0$, thus we get auto-correlation,

$$|R_{SCSS}(\hat{\tau}_1, k_1, k_2) + R_{SCSS}(\hat{\tau}_2, k_1, k_2)| = E_s \quad (20)$$

D. Comparison of SCSS and CSS

From the Fig.3, we use MATLAB to calculate their auto-correlation and cross-correlation with discrete series, when $SF = 6$, and sample interval is $\frac{T}{2}$. It illustrates that maximum cross-correlation of SCSS is smaller than that of CSS. According to (10), (11), (12), (18), (19), (20), and Fig.3, we get three results,

- For cross-correlation, SCSS can make maximum cross-correlation to be less than $0.5E_s$, while CSS is in contrast.
- For auto-correlation, both SCSS and CSS have maximum auto-correlation which is equal to E_s at $\tau = 0$.
- For other τ, the performance of CSS is better than SCSS. In other words, Multiple Access Interference(MAI) of SCSS is bigger than that of CSS.

V. Frequency and Phase Symmetry Chirp Spread Spectrum

Similar with FSK and PSK [10], FSCSS and PSCSS can be applied to communication systems. For Binary FSCSS(BFSCSS), according to (16) and (17), $s_k(t)$ can denote '$1'$('$0'$) and $s'_k(t)$ can denote '$0'$('$1'$). For Binary PSCSS(BPSCSS), we can change the phase of SCSS in order to change completely positive('$0'$) and negative('$1'$) correlation. M-ary FSCSS(MFSCSS) and M-ary PSCSS(MPSCSS), like MFSK and MPSK, can be used to increase data rate in satellite communication systems. As shown in Fig.4, the performance(E_b/N_0-BER) of PSCSS is better than FSCSS under the same SF. When comparing DSSS($SF = 6$) based on BPSK with binary PSCSS($SF = 7$), here we use different values of SF in order to keep the same number of sampling points in one T_s, due to oversampling of PSCSS in our simulations.

VI. Conclusion

In this letter, we analyze the auto-correlation and cross-correlation of CSS and SCSS modulation and find that only SCSS modulation can be applied to LEO satellite communication systems. Finally, we analyze the performance of PSCSS and FSCSS, and find that BPSCSS is as good as DSSS based on BPSK in terms of BER under the situation of no MAI. In further research, we will concentrate upon the methods of decreasing MAI.

References

[1] H. Wang and A. O. Fapojuwo, "A survey of enabling technologies of low power and long range machine-to-machine communications," *IEEE Commun. Surveys Tuts.*, vol. 19, no. 4, pp. 2621–2639, 1st Quart., 2017, doi: 10.1109/COMST.2017.2721379.

[2] *ETSI, Satellite Earth Stations and Systems (SES); Air Interface for S-band Mobile Interactive Multimedia (S-MIM); Part 4: Physical Layer Specification, Return Link Synchronous Access*. [Online]. Available: http://www.etsi.org

[3] (2018). *LoRaWan*. Accessed: Apr. 2018. [Online]. Available: https://lora-alliance.org/sites/default/files/2018-04/lorawantm_specification_-v1.1.pdf

[4] (2018). *LoRa Transceiver*. Accessed: Apr. 2018. [Online]. Available: https://www.semtech.comwireless-rf/rf-transceivers/sx1276

[5] L. Xianbin, C. Li, X. Bo, and Z. Chuansheng, "Study on the method of fast acquisition in LEO satellite DSSS communication system," in *Proc. 10th Int. Conf. Electron. Meas. Instrum. (ICEMI)*, Aug. 2011, pp. 325–328.

[6] L. Vangelista, "Frequency shift chirp modulation: The LoRa modulation," *IEEE Signal Precess. Lett.*, vol. 12, vol. 24, no. 12, pp. 1818–1821, Dec. 2017.

[7] B. Reynders and S. Pollin, "Chirp spread spectrum as a modulation technique for long range communication," in *Proc. Symp. Commun. Veh. Technol. (SCVT)*, Nov. 2016, pp. 1–5.

[8] T. Wang, H. Huang, C. Feng, and R. Tao, "Chirp noise waveform aided fast acquisition approach for large Doppler shifted TT&C system," in *Proc. IEEE Global Commun. Conf. (GLOBECOM)*, Dec. 2015, pp. 1–6.

[9] A. Berni and W. Gregg, "On the utility of chirp modulation for digital signaling," *IEEE Trans. Commun.*, vol. COM-21, no. 6, pp. 748–751, Jun. 1973.

[10] M. A. N. Chowdhury, M. R. U. Mahfuz, S. H. Chowdhury, and M. M. Kabir, "Design of an improved QPSK modulation technique in wireless communication systems," in *Proc. 3rd Int. Conf. Elect. Inf. Commun. Technol. (EICT)*, Dec. 2017, pp. 1–6.